



Published in final edited form as:

Nat Genet. 2012 October ; 44(10): 1126–1130. doi:10.1038/ng.2387.

Common variation at 6q16 within *HACE1* and *LIN28B* influences susceptibility to neuroblastoma

Sharon J Diskin^{1,3}, Mario Capasso^{4,5}, Robert W Schnepf^{1,2}, Kristina A Cole^{1,3}, Edward F Attiye^{1,3}, Cuiping Hou⁶, Maura Diamond^{1,2}, Erica L Carpenter^{1,2}, Cynthia Winter^{1,2}, Hanna Lee^{1,2}, Jayanti Jagannathan^{1,2}, Valeria Latorre^{7,8}, Achille Iolascon^{4,5}, Hakon Hakonarson⁶, Marcella Devoto^{7,9,10}, and John M Maris^{1,3,11}

¹Division of Oncology, Children's Hospital of Philadelphia, Philadelphia, Pennsylvania, USA.

²Center for Childhood Cancer Research, Children's Hospital of Philadelphia, Philadelphia, Pennsylvania, USA.

³Department of Pediatrics, Perelman School of Medicine, University of Pennsylvania, Philadelphia, Pennsylvania, USA.

⁴Dipartimento di Biochimica e Biotecnologie Mediche, Università degli Studi di Napoli "Federico II", Naples, Italy.

⁵Ceinge - Biotecnologie Avanzate, Naples, Italy.

⁶The Center for Applied Genomics, Children's Hospital of Philadelphia, Philadelphia, Pennsylvania, USA.

⁷Division of Genetics, The Children's Hospital of Philadelphia, Philadelphia, Pennsylvania, USA.

⁸Department of Cell Biology, Università della Calabria, Rende, Italy.

⁹University of Rome "La Sapienza", Department of Molecular Medicine, Rome, Italy.

Users may view, print, copy, download and text and data- mine the content in such documents, for the purposes of academic research, subject always to the full Conditions of use: http://www.nature.com/authors/editorial_policies/license.html#terms

Correspondence should be addressed to J.M.M. (maris@chop.edu).

COMPETING FINANCIAL INTEREST The authors declare no competing financial interest.

AUTHOR CONTRIBUTIONS S.J.D and J.M.M. designed the experiment and drafted the manuscript. S.J.D. analyzed SNP data, performed SNP association study and analyzed mRNA and miRNA expression data. M.C. and A.I. replicated SNP associations in Italian cohort. V.L. and M.D. replicated SNP associations in African American cohort. E.L.C. and H.L. confirmed LIN28B protein expression by western blot. R.S. and C.W. performed siRNA knockdown experiments of *LIN28B*. E.F.A. generated miRNA expression array data including low-level summary values. K.A.C. performed RT-PCR in primary tumors. M.D. and C.H. organized samples and genotyped cases. H.H. generated and provided all control data for GWAS. M.D. and H.H. contributed to overall study design. All authors commented on or contributed to the current manuscript.

Accession numbers. The genotyping data are deposited in dbGaP under accession number phs000124.

URLs. dbGaP, <http://www.ncbi.nlm.nih.gov/gap>

LocusZoom, <http://csg.sph.umich.edu/locuszoom>

1000 Genomes Project, <http://www.1000genomes.org>

R2 bioinformatics tool, <http://r2.amc.nl>

NCI Oncogenomics, <http://home.ccr.cancer.gov/oncology/oncogenomics>

EdSumm (same for AOP and issue): John Maris and colleagues identify common variants at 6q16 associated with neuroblastoma susceptibility. The risk variants are located near the *HACE1* and *LIN28B* genes, both of which show altered expression in advanced neuroblastomas.

¹⁰Department of Biostatistics and Epidemiology, Perelman School of Medicine, University of Pennsylvania, Philadelphia, Pennsylvania, USA.

¹¹Abramson Family Cancer Research Institute, Perelman School of Medicine at the University of Pennsylvania, Philadelphia, Pennsylvania, USA.

Abstract

Neuroblastoma is a cancer of the sympathetic nervous system that accounts for approximately 10% of all pediatric oncology deaths¹. Here we report on a genome-wide association study of 2,817 neuroblastoma cases and 7,473 controls. We identified two new associations at 6q16, the first within *HACE1* (rs4336470; combined $P = 2.7 \times 10^{-11}$, odds ratio 1.26, 95% CI: 1.18–1.35) and the second within *LIN28B* (rs17065417; combined $P = 1.2 \times 10^{-8}$, odds ratio 1.38, 95% CI: 1.23–1.54). Expression of *LIN28B* and *let-7* miRNA correlated with rs17065417 genotype in neuroblastoma cell lines, and we observed significant growth inhibition upon depletion of *LIN28B* specifically in neuroblastoma cells homozygous for the risk allele. Low *HACE1* and high *LIN28B* expression in diagnostic primary neuroblastomas were associated with worse overall survival ($P = 0.008$ and 0.014 , respectively). Taken together, we show that common variants in *HACE1* and *LIN28B* influence neuroblastoma susceptibility and that both genes likely play a role in disease progression.

Neuroblastoma is a malignancy derived from the developing sympathetic nervous system. The median age at diagnosis is 17 months, and the survival rate for the most aggressive subset remains approximately 50% despite intensive multi-modal cytotoxic therapy¹ and recent advances in immunotherapy². The genetic etiology of familial neuroblastoma, which accounts for approximately 1% of cases, has recently come into focus³⁻⁶; however, the genetic and environmental factors that cause sporadic neuroblastoma remain largely unknown. We have recently reported common SNPs within or upstream of *LINC00340* and *FLJ44180*, *BARD1*, *LMO1*, *DUSP12*, *HSD17B12* and *DDX4-IL31RA* and a common CNV within *NBPF23* as each being highly associated with neuroblastoma⁷⁻¹¹. Collectively, however, these variants still account for only a small portion of neuroblastoma heritability, and it is likely that additional predisposition loci remain to be discovered.

To identify additional variants associated with neuroblastoma, we expanded our previous genome-wide association study (GWAS) discovery cohort and analyzed 2,101 neuroblastoma cases accrued through the North American-based Children's Oncology Group (Supplementary Table 1) with 4,202 control subjects of European ancestry matched genetically and by genotyping array version to minimize genomic inflation (see Online Methods and Supplementary Figs. 1 and 2). All subjects were genotyped using the Illumina HumanHap550 or Quad610 Beadchip. We restricted our analysis to the SNPs present on both platforms that passed our quality control metrics; the genomic control inflation factor was 1.14 (Supplementary Fig. 3). Evaluation of the first three principal components in cases and controls confirmed that the slightly high inflation factor was not due to gross population stratification (Supplementary Fig. 4). Clusters of SNPs from six genomic loci reached genome-wide significance (P -values ranged from 7.8×10^{-16} to 4.8×10^{-8} ; Supplementary Fig. 1 and Supplementary Table 2), including three SNPs within *LINC00340* and *FLJ44180*

at 6p22 (P -values ranged from 7.8×10^{-16} to 1.7×10^{-14}), ten SNPs within or near *BARD1* at 2q35 (P -values ranged from 4.1×10^{-14} to 3.7×10^{-8}), two SNPs within *LMO1* at 11p15 (P -values ranged from 1.2×10^{-13} to 3.8×10^{-10}) and one SNP within *HSD17B12* at 11p11 ($P = 4.8 \times 10^{-8}$), further confirming our previous reports⁷⁻¹⁰. In addition, we identified one SNP (rs4696715) at chromosome 4p16 and two SNPs (rs4336470 and rs9404576) at 6q16 that have not been reported previously (P -values ranged from 1.8×10^{-8} to 3.4×10^{-8} ; Table 1). Several genotyped SNPs in strong linkage disequilibrium (LD) with rs4696715 at 4p16 did not show evidence for association with neuroblastoma; therefore, this SNP was not considered further here.

Closer examination of the 6q16 locus identified four additional SNPs that showed association ($P < 1 \times 10^{-4}$) with neuroblastoma (Table 1 and Supplementary Table 3). Three of these SNPs mapped to introns of the HECT domain and ankyrin repeat containing, E3 ubiquitin protein ligase 1 gene (*HACE1*) and exhibited a moderate degree of LD with rs4336470. The fourth SNP (rs17065417; $P = 1.8 \times 10^{-7}$) mapped to an intron of the lin-28 homolog B gene (*LIN28B*) and showed very little evidence for LD with rs4336470 in multiple HapMap populations (Supplementary Fig. 5). To ensure these results were not influenced by subtle substructure in the discovery phase, we included the first 20 principal components as covariates in a logistic regression analysis. This reduced the inflation factor to 1.04 but did not alter our conclusions regarding regions reaching genome-wide significance, and the P -values for SNPs at the newly identified 6q16 locus were essentially unchanged (Supplementary Table 4). Finally, we conditioned the analysis of the 6q16 SNPs on rs4336470 to investigate if there might be more than one independent association signal at 6q16. As expected, SNPs in modest LD with rs4336470 were no longer statistically significant after conditioning and clearly represent one signal (Supplementary Table 5). In contrast, while the signal at rs17065417 was attenuated, it remained significant ($P = 2.5 \times 10^{-4}$; Supplementary Table 5), suggesting that rs4336470 and rs17065417 may contribute independently to neuroblastoma risk. No association was observed between rs4336470 or rs17065417 genotypes and clinical or biological covariates (Supplementary Tables 6 and 7), and we observed only weak evidence for epistasis at the other significant loci (Supplementary Tables 8 and 9), suggesting that each may act independently to confer risk.

We next sought to replicate the rs4336470 and rs17065417 associations in an Italian cohort of 351 cases and 780 controls using PCR-based genotyping. Both SNPs showed evidence for association in the same direction seen in the discovery effort (Table 1 and Supplementary Table 3). To assess whether these variants influence susceptibility in other ethnic groups, and to seek additional replication, we analyzed a third independent case series comprised of 365 African American neuroblastoma cases and 2,491 genetically matched controls, all genotyped on the Illumina HumanHap550 or Quad610 BeadChip. After accounting for African admixture in logistic regression analysis, the genomic inflation factor was 1.02, as described previously¹² (Online Methods and Supplementary Fig. 6). Consistent with the lower incidence rate of neuroblastoma in African Americans¹³, the rs4336470 protective allele (T) is actually the major allele in African Americans, whereas it is the minor allele in individuals of European ancestry. Despite these observed differences in allele frequencies, all SNPs mapped to *HACE1* replicated robustly in the African American cohort

(P -values ranged from 1.3×10^{-4} to 1.4×10^{-3} ; Table 1 and Supplementary Table 3), and all associations were in the same direction. Allele frequencies for the *LIN28B* SNP rs17065417 were comparable across ethnic populations and showed a trend toward association in African Americans in the same direction as the European American discovery and Italian replication cohorts (Table 1 and Supplementary Table 3). Combined analysis using the weighted inverse-variance method in METAL¹⁴ demonstrated that all six genotyped SNPs had P values beyond or approaching the conservative Bonferroni adjusted genome-wide significance threshold (P -values ranged from 2.7×10^{-11} to 1.6×10^{-7} ; Table 1).

To identify variants at the 6q16 locus not assayed directly on the Illumina SNP arrays, we performed genotype imputation in our discovery cohort using data from the 1000 Genomes project. This analysis identified ten additional genome-wide significant SNPs (P -values ranged from 4.4×10^{-9} to 5.7×10^{-8} ; Fig. 1). Five of these imputed SNPs were in strong LD with rs4336470 ($r^2 > 0.8$ in 1000 Genomes EUR population); three mapped to introns of *HACE1* and the other two were located just downstream of *HACE1* (Fig. 1a). The remaining five imputed SNPs reaching genome-wide significance were in strong LD with rs17065417 ($r^2 > 0.8$ in 1000 Genomes EUR population) and were located within introns of *LIN28B* (Fig. 1b). In total, we identified 46 imputed SNPs that showed strong evidence for association ($P < 1.0 \times 10^{-6}$, Supplementary Table 10). To further evaluate whether two independent association signals exist at 6q16, we conditioned the regional association analysis on either rs4336470 or rs17065417 and found that neither could fully account for the observed associations (Supplementary Fig. 7). The signal at 6q16 was only abolished across the entire region after conditioning on both rs4336470 and rs17065417 (Supplementary Fig. 8). While we cannot rule out the possibility that both SNPs may be tagging the same underlying risk variant, these data are consistent with the presence of two independent association signals at 6q16, one implicating *HACE1* and the other *LIN28B*.

The *HACE1* gene encodes an E3 ubiquitin-protein ligase that was first identified in a sporadic Wilms tumor that harbored a t(6;15)(q21;q21) translocation¹⁵. The rearrangement was associated with decreased *HACE1* expression, and further study showed that *HACE1* is silenced in the majority of Wilms tumors via hypermethylation of two CpG islands upstream of the transcriptional start site¹⁵. Similar epigenetic silencing has been reported in advanced colorectal cancer¹⁶ and gastric carcinoma¹⁷. Indeed *HACE1* is down-regulated in multiple human tumors and maps to a region of common deletion or LOH, consistent with a tumor suppressor function. *Hace1* null mice form spontaneous tumors in a wide array of tissues and are susceptible to additional cancer triggers, both genetic and environmental¹⁸. Through its E3 ubiquitin ligase function, *HACE1* has been shown to suppress cell growth and anchorage independence of human tumor cells, including the neuroblastoma cell line IMR32 (ref. 18). Studies suggest that *HACE1* inhibits cell cycle progression during stress via regulation of cyclin D1 degradation¹⁸ and that *HACE1* also regulates retinoic acid receptor (RAR) activity¹⁹. In addition to multiple somatic alterations involving the *HACE1* locus, a constitutional t(5;6)(q21;q21) translocation that disrupts *HACE1* was recently identified, making it a putative Wilms tumor susceptibility gene²⁰.

The *LIN28B* gene encodes a developmentally regulated RNA binding protein and is a key repressor of the let-7 family of microRNAs²¹. Both *LIN28A* and *LIN28B* function as oncogenes that promote cellular transformation when ectopically over-expressed²²⁻²⁴, and high levels of expression of *LIN28A* or *LIN28B* have been observed in several human cancers and correlate with low let-7 levels^{22,24}. Post-transcriptional regulation of let-7 by *LIN28A* is required for normal development and contributes to the pluripotent state by preventing let-7-mediated differentiation of embryonic stem cells^{21,25,26}. Over-expressing *LIN28* or inhibiting let-7 with antisense RNA promotes reprogramming of human and mouse fibroblast to pluripotent stem cells^{26,27}. In a panel of 60 pediatric cancer cell lines²⁸, *LIN28B* was consistently expressed at high levels in neuroblastoma (Supplementary Fig. 9). Recently, *LIN28B* and *let-7* were also identified as key regulators of glucose homeostasis²⁹ and hematopoiesis³⁰. To date, GWAS studies have identified variants in *LIN28B* associated with human height³¹ and the age of onset of puberty³² and menarche³³. In addition, a recent candidate gene study identified a putative association with epithelial ovarian cancer³⁴.

To investigate the functional relevance of neuroblastoma-associated SNPs within *HACE1* and *LIN28B*, we first analyzed a set of 12 neuroblastoma cell lines with matched genome-wide SNP genotyping and mRNA expression data. No correlation between rs4336470 and *HACE1* mRNA expression was observed ($P = 0.30$), but *LIN28B* expression was significantly higher in cell lines homozygous for the rs17065417 risk allele (A) compared to heterozygous cell lines ($P = 0.02$; Fig. 2a). No cell lines tested were homozygous for the rs17065417 protective allele (C). *LIN28A* was not expressed in neuroblastoma cell lines, consistent with recent reports that *LIN28A* and *LIN28B* may be mutually exclusive in terms of their expression in cancer cells²¹. In addition to a correlation between rs17065417 genotype and *LIN28B* expression, we observed a strong positive correlation with *MYCN* expression ($P = 0.0003$; Fig. 2b). We next confirmed *LIN28B* protein levels by western blot in four cell lines at the extremes of *LIN28B* mRNA expression (Fig. 2c). Cell lines expressing high *LIN28B* showed lower let-7 expression across the entire miRNA family (Fig. 2d). Transient knockdown of *LIN28B* resulted in significant growth inhibition in neuroblastoma cells homozygous for the rs17065417 risk allele and with high *LIN28B* expression (Fig. 3a-d), but not in the heterozygous cell line SKNAS with low *LIN28B* expression (Fig. 3e,f). Taken together, these data are consistent with the hypothesis that *LIN28B* promotes neuroblastoma tumorigenesis in part through repression of let-7 miRNAs, and that the risk alleles are associated with growth advantage through increased *LIN28B* expression; however, additional studies with larger sample sizes are needed to confirm this.

To examine the relevance of *HACE1* and *LIN28B* in tumor samples, we assayed expression of both genes by real-time quantitative RT-PCR in a representative set of 87 primary tumors obtained at time of diagnosis (Supplementary Table 1). *HACE1* expression was significantly lower ($P = 0.002$; Fig. 4a) and *LIN28B* expression was significantly higher ($P = 0.032$; Fig. 4b) in the high-risk tumors. Accordingly, low *HACE1* expression was associated with a worse overall survival ($P = 0.008$; Fig. 4c), as was high *LIN28B* expression ($P = 0.015$; Fig. 4d). Analysis of four independent mRNA expression array datasets comprising 517 neuroblastoma tumors provided robust replication of these observations (Fig. 4e-h and

Supplementary Figs. 10-12). These data support the hypothesis that *HACE1* may function as a tumor suppressor, and *LIN28B* as an oncogene, in advanced neuroblastomas.

In conclusion, here we have identified common variants within *HACE1* and *LIN28B* that are associated with neuroblastoma. Similar to other genes identified in our ongoing GWAS efforts^{8,9,35}, it is likely that the germline susceptibility variants identified here play an important role not only in tumor initiation but also in disease progression via *cis*-effects on major cancer genes. Further study of *HACE1* and *LIN28B* in neuroblastoma is warranted and may lead to new insights into the genetic and epigenetic mechanisms underlying an aggressive clinical phenotype.

Supplementary Material

Refer to Web version on PubMed Central for supplementary material.

ACKNOWLEDGMENTS

This work was supported in part by NIH Grants R01-CA124709 (J.M.M.), K99-CA151869 (S.J.D.), P30-HD026979 (M.D.), the Giulio D'Angio Endowed Chair (J.M.M.), the Alex's Lemonade Stand Foundation (J.M.M.), Andrew's Army Foundation (J.M.M.), the PressOn Foundation (J.M.M.), the Abramson Family Cancer Research Institute (J.M.M.), K08-CA136979 (K.A.C.), *Fondazione* Italiana per la Lotta al *Neuroblastoma* and Associazione Italiana per la Ricerca sul Cancro (M.C.) and the Center for Applied Genomics at the Children's Hospital of Philadelphia Research Institute (H.H.). We thank Patrick Sleiman for useful discussions regarding meta-analysis using METAL.

REFERENCES

1. Maris JM. Recent advances in neuroblastoma. *N. Engl. J. Med.* 2010; 362:2202–2211. [PubMed: 20558371]
2. Yu AL, et al. Anti-GD2 antibody with GM-CSF, interleukin-2, and isotretinoin for neuroblastoma. *N. Engl. J. Med.* 2010; 363:1324–1334. [PubMed: 20879881]
3. Mosse YP, et al. Identification of *ALK* as a major familial neuroblastoma predisposition gene. *Nature.* 2008; 455:930–935. [PubMed: 18724359]
4. Janoueix-Lerosey I, et al. Somatic and germline activating mutations of the *ALK* kinase receptor in neuroblastoma. *Nature.* 2008; 455:967–970. [PubMed: 18923523]
5. Trochet D, et al. Germline mutations of the paired-like homeobox 2B (*PHOX2B*) gene in neuroblastoma. *Am. J. Hum. Genet.* 2004; 74:761–764. [PubMed: 15024693]
6. Mosse YP, et al. Germline *PHOX2B* mutation in hereditary neuroblastoma. *Am. J. Hum. Genet.* 2004; 75:727–730. [PubMed: 15338462]
7. Maris JM, et al. Chromosome 6p22 locus associated with clinically aggressive neuroblastoma. *N. Engl. J. Med.* 2008; 358:2585–2593. [PubMed: 18463370]
8. Capasso M, et al. Common variations in *BARD1* influence susceptibility to high-risk neuroblastoma. *Nat. Genet.* 2009; 41:718–723. [PubMed: 19412175]
9. Wang K, et al. Integrative genomics identifies *LMO1* as a neuroblastoma oncogene. *Nature.* 2010; 469:216–220. [PubMed: 21124317]
10. Nguyen LB, et al. Phenotype restricted genome-wide association study using a gene-centric approach identifies three low-risk neuroblastoma susceptibility loci. *PLoS Genet.* 2011; 7:e1002026. [PubMed: 21436895]
11. Diskin SJ, et al. Copy number variation at 1q21.1 associated with neuroblastoma. *Nature.* 2009; 459:987–991. [PubMed: 19536264]
12. Latorre V, et al. Replication of neuroblastoma SNP association at the *BARD1* locus in African-Americans. *Cancer Epidemiol. Biomarkers Prev.* 2012; 21:658–663. [PubMed: 22328350]

13. Henderson TO, et al. Racial and ethnic disparities in risk and survival in children with neuroblastoma: a Children's Oncology Group study. *J. Clin. Oncol.* 2010; 29:76–82. [PubMed: 21098321]
14. Willer CJ, Li Y, Abecasis GR. METAL: fast and efficient meta-analysis of genomewide association scans. *Bioinformatics.* 2010; 26:2190–2191. [PubMed: 20616382]
15. Anglesio MS, et al. Differential expression of a novel ankyrin containing E3 ubiquitin-protein ligase, Hace1, in sporadic Wilms' tumor versus normal kidney. *Hum. Mol. Genet.* 2004; 13:2061–2074. [PubMed: 15254018]
16. Hibi K, et al. Aberrant methylation of the *HACE1* gene is frequently detected in advanced colorectal cancer. *Anticancer Res.* 2008; 28:1581–1584. [PubMed: 18630515]
17. Sakata M, et al. Methylation of *HACE1* in gastric carcinoma. *Anticancer Res.* 2009; 29:2231–2233. [PubMed: 19528486]
18. Zhang L, et al. The E3 ligase HACE1 is a critical chromosome 6q21 tumor suppressor involved in multiple cancers. *Nat. Med.* 2007; 13:1060–1069. [PubMed: 17694067]
19. Zhao J, Zhang Z, Vucetic Z, Soprano KJ, Soprano DR. HACE1: A novel repressor of RAR transcriptional activity. *J. Cell. Biochem.* 2009; 107:482–493. [PubMed: 19350571]
20. Slade I, et al. Constitutional translocation breakpoint mapping by genome-wide paired-end sequencing identifies *HACE1* as a putative Wilms tumour susceptibility gene. *J. Med. Genet.* 2009; 47:342–347. [PubMed: 19948536]
21. Piskounova E, et al. Lin28A and Lin28B inhibit let-7 microRNA biogenesis by distinct mechanisms. *Cell.* 2011; 147:1066–1079. [PubMed: 22118463]
22. Iliopoulos D, Hirsch HA, Struhl K. An epigenetic switch involving NF- κ B, Lin28, Let-7 microRNA, and IL6 links inflammation to cell transformation. *Cell.* 2009; 139:693–706. [PubMed: 19878981]
23. West JA, et al. A role for Lin28 in primordial germ-cell development and germ-cell malignancy. *Nature.* 2009; 460:909–913. [PubMed: 19578360]
24. Viswanathan SR, et al. Lin28 promotes transformation and is associated with advanced human malignancies. *Nat. Genet.* 2009; 41:843–848. [PubMed: 19483683]
25. Martinez NJ, Gregory RI. MicroRNA gene regulatory pathways in the establishment and maintenance of ESC identity. *Cell Stem Cell.* 2010; 7:31–35. [PubMed: 20621047]
26. Melton C, Judson RL, Blelloch R. Opposing microRNA families regulate self-renewal in mouse embryonic stem cells. *Nature.* 2010; 463:621–626. [PubMed: 20054295]
27. Yu J, et al. Induced pluripotent stem cell lines derived from human somatic cells. *Science.* 2007; 318:1917–1920. [PubMed: 18029452]
28. Neale G, et al. Molecular characterization of the pediatric preclinical testing panel. *Clin. Cancer Res.* 2008; 14:4572–4583. [PubMed: 18628472]
29. Zhu H, et al. The Lin28/let-7 axis regulates glucose metabolism. *Cell.* 2011; 147:81–94. [PubMed: 21962509]
30. Yuan J, Nguyen CK, Liu X, Kanellopoulou C, Muljo SA. Lin28b reprograms adult bone marrow hematopoietic progenitors to mediate fetal-like lymphopoiesis. *Science.* 2012; 335:1195–1200. [PubMed: 22345399]
31. Widen E, et al. Distinct variants at *LIN28B* influence growth in height from birth to adulthood. *Am. J. Hum. Genet.* 2010; 86:773–782. [PubMed: 20398887]
32. Ong KK, et al. Genetic variation in *LIN28B* is associated with the timing of puberty. *Nat. Genet.* 2009; 41:729–733. [PubMed: 19448623]
33. Sulem P, et al. Genome-wide association study identifies sequence variants on 6q21 associated with age at menarche. *Nat. Genet.* 2009; 41:734–738. [PubMed: 19448622]
34. Permut-Wey J, et al. *LIN28B* polymorphisms influence susceptibility to epithelial ovarian cancer. *Cancer Res.* 2011; 71:3896–3903. [PubMed: 21482675]
35. Bosse KR, et al. Common variation at *BARD1* results in the expression of an oncogenic isoform that influences neuroblastoma susceptibility and oncogenicity. *Cancer Res.* 2012; 72:2068–2078. [PubMed: 22350409]

36. Pruim RJ, et al. LocusZoom: regional visualization of genome-wide association scan results. *Bioinformatics*. 2010; 26:2336–2337. [PubMed: 20634204]
37. Brodeur GM, et al. Revisions of the international criteria for neuroblastoma diagnosis, staging, and response to treatment. *J. Clin. Oncol.* 1993; 11:1466–1477. [PubMed: 8336186]
38. Shimada H, et al. The International Neuroblastoma Pathology Classification (Shimada) System. *Cancer*. 1999; 86:364–372. [PubMed: 10421273]
39. Mathew P, et al. Detection of *MYCN* gene amplification in neuroblastoma by fluorescence *in situ* hybridization: a Pediatric Oncology Group study. *Neoplasia*. 2001; 3:105–109. [PubMed: 11420745]
40. Look AT, et al. Clinical relevance of tumor cell ploidy and *N-myc* gene amplification in childhood neuroblastoma: a Pediatric Oncology Group study. *J. Clin. Oncol.* 1991; 9:581–591. [PubMed: 2066755]
41. Gunderson KL, Steemers FJ, Lee G, Mendoza LG, Chee MS. A genome-wide scalable SNP genotyping assay using microarray technology. *Nat. Genet.* 2005; 37:549–554. [PubMed: 15838508]
42. Steemers FJ, et al. Whole-genome genotyping with the single-base extension assay. *Nat. Methods*. 2006; 3:31–33. [PubMed: 16369550]
43. Howie BN, Donnelly P, Marchini J. A flexible and accurate genotype imputation method for the next generation of genome-wide association studies. *PLoS Genet.* 2009; 5:e1000529. [PubMed: 19543373]
44. Howie B, Marchini J, Stephens M. Genotype imputation with thousands of genomes. *G3*. 2011; 1:457–470. [PubMed: 22384356]
45. Marchini J, Howie B, Myers S, McVean G, Donnelly P. A new multipoint method for genome-wide association studies by imputation of genotypes. *Nat. Genet.* 2007; 39:906–913. [PubMed: 17572673]
46. Cole KA, et al. A functional screen identifies miR-34a as a candidate neuroblastoma tumor suppressor gene. *Mol. Cancer Res.* 2008; 6:735–742. [PubMed: 18505919]
47. Kaplan EL, Meier P. Nonparametric estimation from incomplete observations. *J. Am. Stat. Assn.* 1958; 53:457–481.

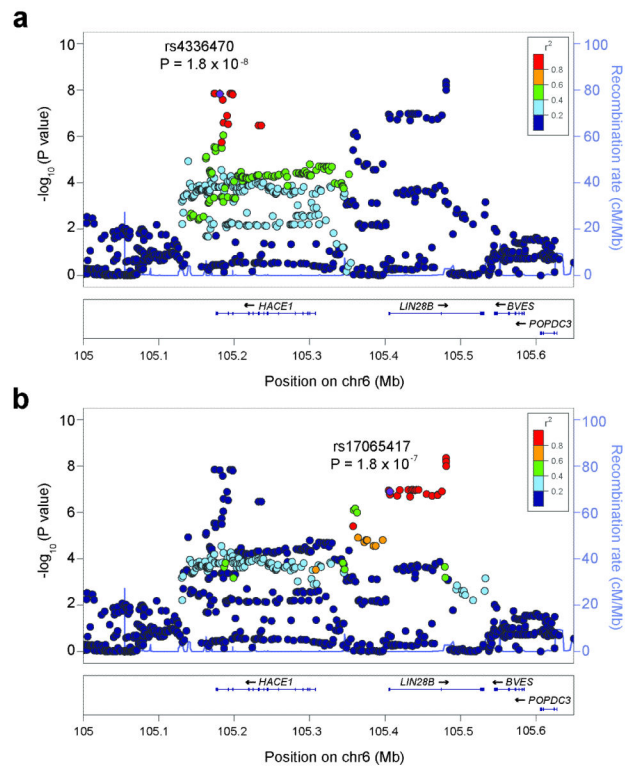


Figure 1.

Regional association plots at the *HACE1* and *LIN28B* loci. Regional association plots including both genotyped and imputed SNPs for the *HACE1* and *LIN28B* loci generated by LocusZoom³⁶. Plotted are the significance of association ($-\log_{10}$ transformed P values) and the recombination rate. SNPs are color-coded based on pair-wise linkage disequilibrium (r^2) with the most significant genotyped SNP in the EUR (European) 1000 Genomes Interim Phase I release genotypes. The most significant genotyped SNP and associated P -value are labeled, and the SNP is shown in purple. (a) *HACE1* locus (b) *LIN28B* locus.

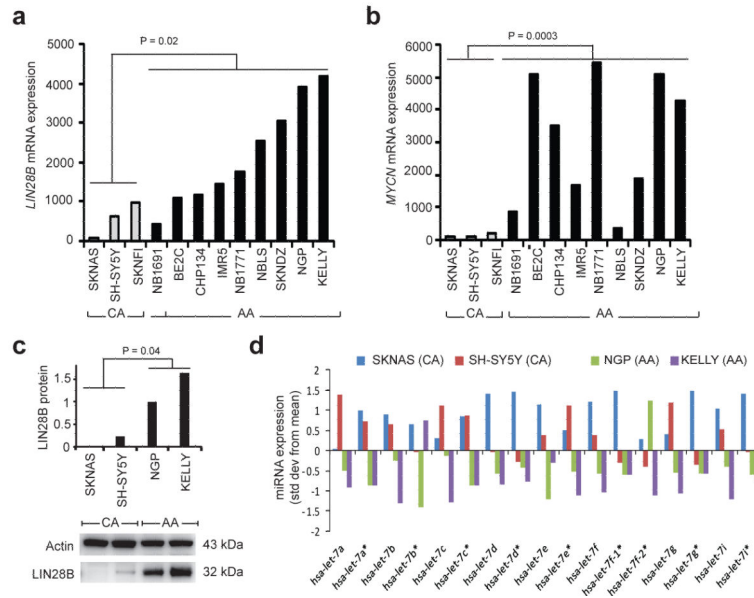


Figure 2. *LIN28B* risk alleles correlate with increased *LIN28B* expression and decreased *let-7* miRNA expression. (a) *LIN28B* mRNA expression is significantly higher in neuroblastoma cell lines homozygous for the rs17065417 risk allele (AA) compared to neuroblastoma cell lines heterozygous for the risk allele (CA). Given the MAF of rs17065417, we did not identify any cell lines homozygous for the protective allele (CC). (b) Neuroblastoma cell lines homozygous for the rs17065417 risk allele show high expression of *MYCN*. (c) Western blot confirms increased protein expression of *LIN28B* in neuroblastoma cell lines homozygous for the rs17065417 risk allele. (d) Neuroblastoma cell lines homozygous for the rs17065417 risk allele and with high *LIN28B* expression show decreased or absent expression of the *let-7* miRNAs.

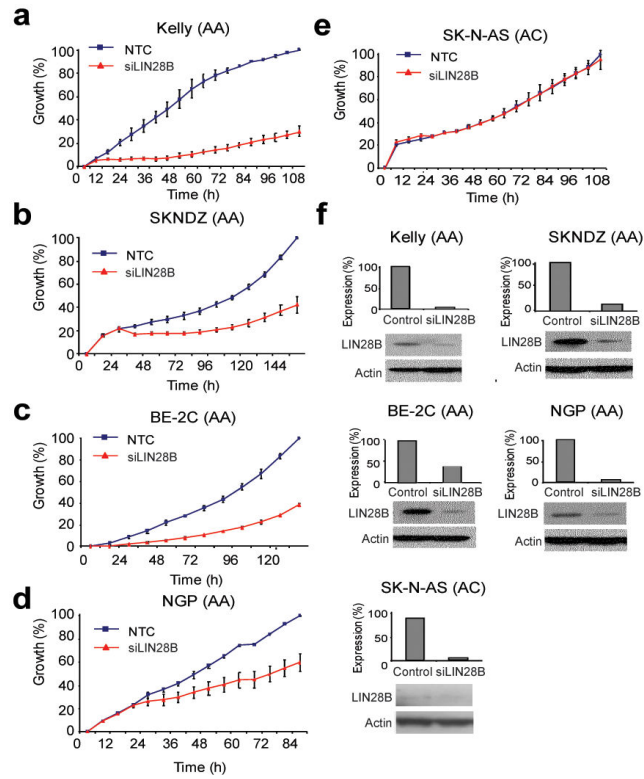


Figure 3.

Transient knockdown of *LIN28B* influences neuroblastoma cell growth in an expression-specific manner. (a-d) In cells homozygous for neuroblastoma risk alleles and with higher *LIN28B* expression levels, *LIN28B* knockdown leads to significant growth inhibition. (e) In cells heterozygous for the risk allele (carrying one protective allele) and with low *LIN28B* expression, *LIN28B* knockdown does not affect cell growth. (f) *LIN28B* knockdown as measured by quantitative reverse transcription PCR and western blot for experiments a-e.

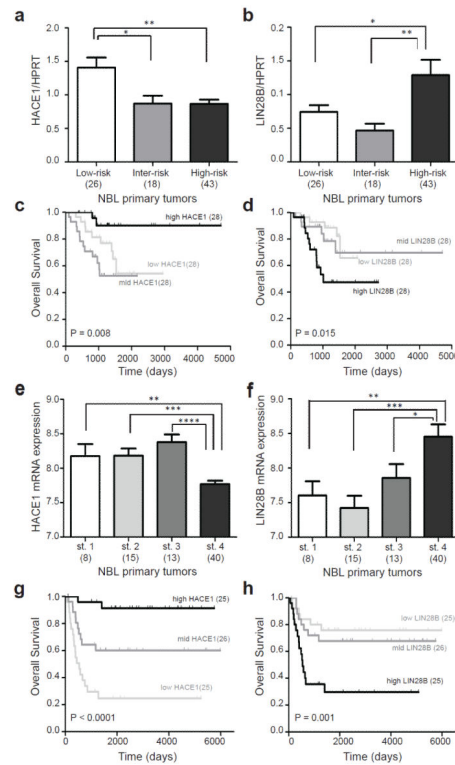


Figure 4.

HACE1 and *LIN28B* expression are associated with advanced disease and poor outcome in neuroblastoma. (a) *HACE1* mRNA expression is significantly lower in high-risk neuroblastoma tumors. Bar graph is shown for Children's Oncology Group (COG) risk groups. (error bars: s.e.m.). (b) *LIN28B* mRNA expression is significantly increased in high-risk neuroblastoma tumors. Bar graph is shown for Children's Oncology Group (COG) risk groups. (error bars: s.e.m.). (c) Decreased *HACE1* expression in primary tumors obtained at diagnosis is associated with worse overall survival. Kaplan-Meier analysis is shown, with patients grouped by tertiles of *HACE1* expression. Log rank *P*-value is shown. (d) Increased *LIN28B* expression in primary tumors obtained at diagnosis is associated with worse overall survival. Kaplan-Meier analysis is shown, with patients grouped by tertiles of *LIN28B* expression. Log rank *P*-value is shown. (e) Replication of decreased *HACE1* in advanced stage neuroblastoma using published Affymetrix U133 plus v2 array data (R2 bioinformatics tool). Bar graph is shown for INSS stage 1-4 (error bars: s.e.m.). (f) Replication of increased *LIN28B* in advanced stage neuroblastoma (R2 bioinformatics tool). Bar graph is shown for INSS stage 1-4 (error bars: s.e.m.). (g) Decreased expression of *HACE1* is associated with worse outcome in dataset from e. Kaplan-Meier analysis is shown, with patients grouped by tertiles of *HACE1* expression. Log rank *P*-value is shown. (h) Increased expression of *LIN28B* is associated with worse outcome in dataset from f. Kaplan-Meier analysis is shown, with patients grouped by tertiles of *LIN28B* expression. Log rank *P*-value is shown. *****P* < 0.0001, ****P* < 0.001, ***P* < 0.01, **P* < 0.05.

Table 1

Significantly associated genotyped SNPs at the *HACE1* and *LIN28B* loci at 6q16

| SNP | A1/A2 (protective/ risk allele) | Discovery cohort ^d European ancestry | | | | Italian replication ^d (TaqMan) | | | CHOP replication ^d African American | | | Combined | |
|---------------|---------------------------------------|--|------------------------------------|------------------------|-------------------------------|--|----------------|-------------------------------|---|------------------------|-------------------------|--|--|
| | | Freq A1 cases (n = 2,101) | Freq A1 controls (n = 4,202) | P ^b | Freq A1 cases (n = 351) | Freq A1 controls (n = 780) | P ^b | Freq A1 cases (n = 365) | Freq A1 controls (n = 2,491) | P ^c | Meta P ^d | OR ^e (95% CI) ^f | |
| <i>HACE1</i> | | | | | | | | | | | | | |
| rs4336470 | T/C | 0.30 | 0.35 | 1.8 × 10 ⁻⁸ | 0.30 | 0.34 | 0.060 | 0.62 | 0.70 | 1.4 × 10 ⁻³ | 2.7 × 10 ⁻¹¹ | 1.26 (1.18–1.35) | |
| rs9404576 | G/T | 0.30 | 0.35 | 3.4 × 10 ⁻⁸ | - | - | - | 0.62 | 0.70 | 1.3 × 10 ⁻³ | 1.8 × 10 ⁻¹⁰ | 1.27 (1.18–1.36) | |
| rs4079063 | G/A | 0.43 | 0.47 | 4.0 × 10 ⁻⁵ | - | - | - | 0.70 | 0.78 | 1.3 × 10 ⁻⁴ | 1.3 × 10 ⁻⁷ | 1.20 (1.12–1.29) | |
| rs2499663 | C/T | 0.43 | 0.47 | 4.5 × 10 ⁻⁵ | - | - | - | 0.70 | 0.78 | 1.5 × 10 ⁻⁴ | 1.6 × 10 ⁻⁷ | 1.21 (1.13–1.29) | |
| rs2499667 | G/A | 0.43 | 0.47 | 2.6 × 10 ⁻⁵ | - | - | - | 0.71 | 0.78 | 2.6 × 10 ⁻⁴ | 1.2 × 10 ⁻⁷ | 1.21 (1.13–1.29) | |
| <i>LIN28B</i> | | | | | | | | | | | | | |
| rs17065417 | C/A | 0.08 | 0.11 | 1.8 × 10 ⁻⁷ | 0.08 | 0.11 | 0.033 | 0.09 | 0.11 | 0.129 | 1.2 × 10 ⁻⁸ | 1.38 (1.23–1.54) | |

^aNo deviations from Hardy-Weinberg equilibrium were observed ($P > 0.001$) in all cohorts.^bP-values were calculated by allelic test.^cP-values were calculated by logistic regression with percent African admixture as covariate¹².^dMeta-analysis P-value calculated using METAL¹⁴.^eOR, odds ratio of risk allele based on meta-analysis.^fCI, confidence interval.